CHAPTER III

Result and discussion

3.1 Experimental conditions to observe PNA-DNA duplexes

In recent year, pyrrolidinyl PNA with alpha/beta-dipeptide backbone of prolyl-2-aminocyclopentane-carboxylic acid (acpcPNA) have been developed by Vilaivan et al [43, 44]. Several properties of acpcPNA have been improved from the original PNA (aegPNA) such as thermal stability, specificity and non-self-pairing ability. In this study, a nine base homothymine acpcPNA (pT_9) was used as a model to optimize the ESI-MS conditions because it is the most simple and shortest sequence that can exhibit a good thermal stability (T_m = 80 ^{0}C) when hybridized with its complementary DNA (dA_9). The high thermal stability means that the pT_9-dA_9 hybrid should be very stable at room temperature and thus should be a good model for studying of non-covalent interaction by mass spectrometry. Initially, we have optimized the conditions for PNA ionization from the electrospray ionization source. The pT_9-dA_9 stock samples were prepared by mixing the two components together at a concentration of 10 uM in different water/acetonitrile ratios at 90:10, 80:20, 70:30 and 60:40. All samples were infused into MS ionization source with a flow rate 180 uL/h and the capillary voltage was set to 2.5 kV. The source temperature was adjusted to 180 °C and the source pressure was set at 0.4 bar. The end plate offset was set to -500 V. Full scan MS spectra were recorded in the m/z range between 300 and 3000. Data were analyzed using the Compass Data analysis software developed by Bruker (German). Adding a small amount of an organic solvent (acetonitrile) enhanced the electrospray ionization however, high concentration of acetonitrile leading to the signal suppression. The sample prepared in water/acetonitrile at a ratio of 90:10 generated the highest intensity of the PNA-DNA complexes. Figure 3.1 showed the multiple charged ions of pT_9-dA_9 complex and the single strand dA_9.

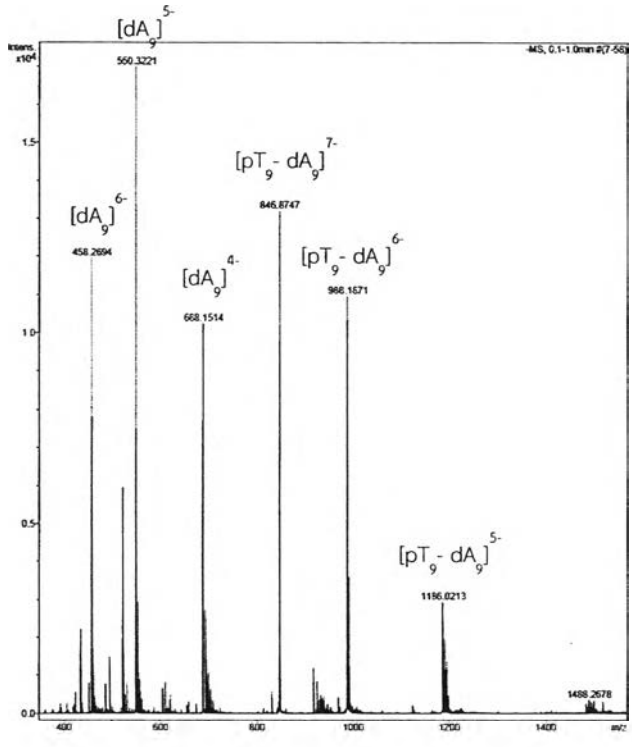

Figure 3.1 ESI mass spectra of pT_9-dA_9 prepared in water:acetonitrile 90:10 showing the multiple charged pT_9-dA_9 duplexes and single stranded dA_9.

All peaks in Figure 3.1 can be assigned as $[pT_9\text{-}dA_9\text{-}5H]^{5-}$, $[pT_9\text{-}dA_9\text{-}6H]^{6-}$, $[pT_9\text{-}dA_9\text{-}7H]^{7-}$, $[dA_9\text{-}4H]^{4-}$, $[dA_9\text{-}5H]^{5-}$ and $[dA_9\text{-}6H]^{6-}$ at m/z = 1185.3940, 987.6680, 846.4231, 687.8854, 550.1149 and 458.2694, respectively. According to this MS spectrum, the experimental molecular mass of pT_9-dA_9 complex was 5932.0408 Da ± 1.8711 ppm. The stability the non-covalently associated pT_9-dA_9 complex was determined from the E_{CM} value of the collision induce dissociation (CID) in Figure 3.2.

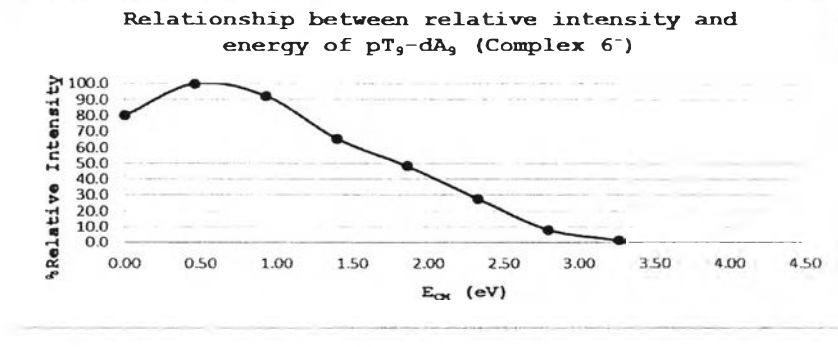

Figure 3.2 Relationship between dissociation energy (E_{CM}) and intensity of pT_9-dA_9.

From the Figure 3.2, the E_{CM} value that could completely dissociate the duplex is 3.2648 eV. This is the dissociation energy of the noncovalent interaction between pT_9 and dA_9. In principle, increasing the energy should result in decreased signals due to dissociation of the PNA-DNA complex. However, from 0-2 eV, the intensity of PNA-DNA complex appeared to increase. This can be explained by the transfer of the inner energy from collision gas that increases the inner energy of PNA-DNA complexes. After the inner energy of complex was increased, the energy is distributed and return to the collision gas after the collision gas moves closer to the complex ion. The inner energy of complex was distributed to collision gas, thus increasing the stability of the complex and the measured intensity is increased [27].

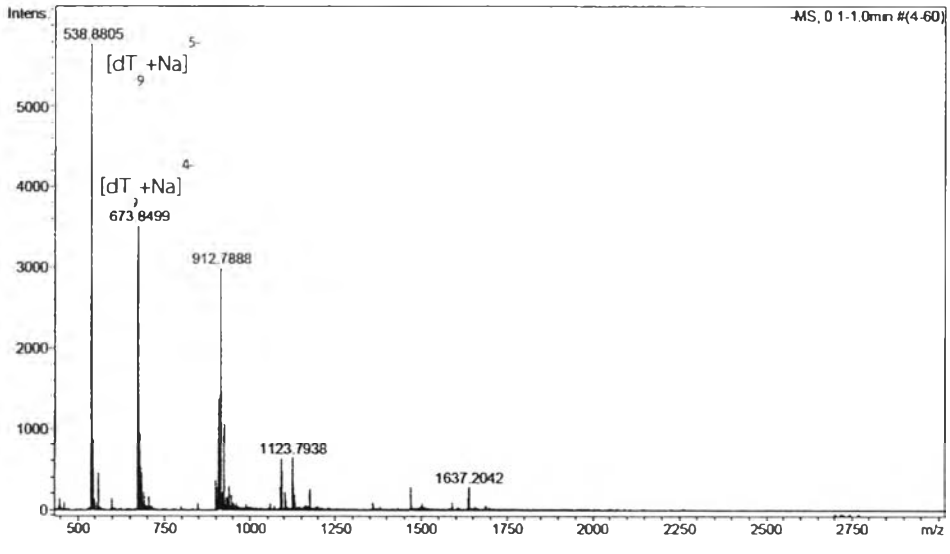

Figure 3.3 ESI mass spectra of pT_9-dT_9 prepared in water: acetonitrile 90:10.

From Figure 3.3, the specificity of PNA-DNA hybridization was studied by using pT_9-dA_9 complex. This spectra was used to confirm the specificity hybridized between acpcPNA with complementary DNA. From this spectrum, we find that the single strand of DNA only and no peak of PNA-DNA complex. This is because the PNA (pT_9) does not binding with DNA (dT_9). So the system of acpcPNA have more specificity with the complementary DNA.

3.2. Analyses of mass spectra of PNA-DNA duplexes

The ratio of solvent was applied to study the stability of various acpcPNA-DNA duplexes. The sequence of the PNA was divided into two sets. The first set contains four 12 mer PNA with almost identical sequence, with the exception of the bases at positions 4 and 7 (denoted by underlining in Table 3.1). The second set contains two random G-C rich PNA sequences that contain more than 70% G-C. The sequences of all acpcPNA and its complementary DNA are shown in Table 3.1.

Table 3.1 Sequences and other properties of PNA and DNA used in the experiment.

PNA/DNA no.	PNA[a]/DNA[b] Seq.	MW.	%G+C
p01 (TT)	TGT TAATTG ACT	4296.9766	25
d01 (AA)	ACA ATTAAC TGA	3635.6726	25
P02 (AA)	TGT AAAATG ACT	4314.9997	25
D02 (TT)	ACA TTTTAC TGA	3617.6495	25
p03 (CC)	TGT CAACTG ACT	4266.9773	41
d03 (GG)	ACA GTTGAC TGA	3627.6563	41
p04 (GG)	TGT GAAGTG ACT	4346.9896	41
d04 (CC)	ACA CTTCAC TGA	3587.6502	41
p_05	CGC GCTCCG CTA	4228.9821	75
d_05	GCG CGAGGC GAT	3709.6714	75
p_06	CGC GCAGGT TCC	4268.9883	75
d_06	GCG CGTCCA AGG	3669.6536	75

[a]The PNA sequences are written from the N- to C-terminus. All sequences carried an N-benzoyl and C-lysinamide end-caps.

[b]The DNA sequences are written from the 3' to 5'.

The experiments were designed to study the noncovalent interactions in PNA-DNA complexes by ESI-MS. In the first set of PNA-DNA complexes, only the bases at the position 4 and 7 were different, therefore the effect of different base pairs to the stability can be systematically compared. The ESI-MS spectra of first set PNA-DNA complexes are shown in Figure 3.4 - Figure 3.7. The spectra of the second set of PNA-DNA complexes are shown in Figure 3.8 - Figure 3.9.

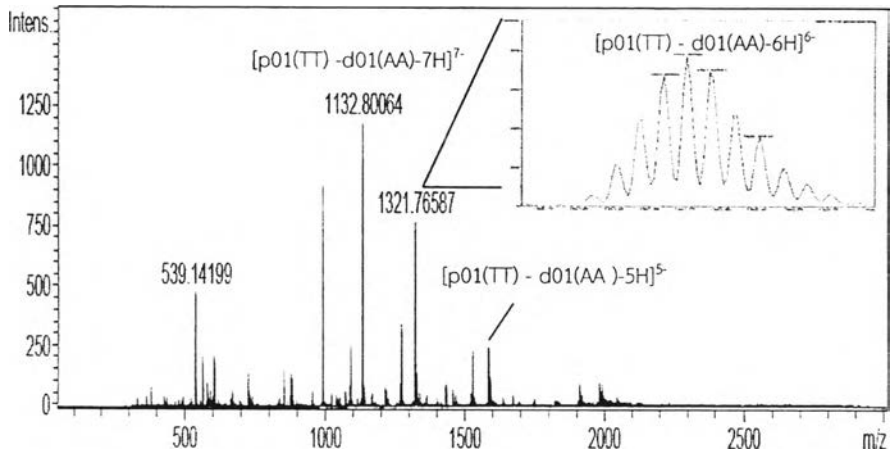

Figure 3.4 Mass spectra of p01 (TT) -d01 (AA) duplex, showing the multiple charged species obtained.

According to this MS spectrum, the experimental molecular mass of p01(TT)–d01(AA) complex was 7932.6762 Da ± 3.4036 ppm. The peaks in Figure 3.4 at m/z = 1586.3223, 1321.7658 and 1132.8006 can be interpreted as $[p01(TT)\text{-}d01(AA)\text{-}5H]^{5-}$, $[p01(TT)\text{-}d01(AA)\text{-}6H]^{6-}$ and $[p01(TT)\text{-}d01\ (AA)\text{-}7H]^{7-}$ respectively.

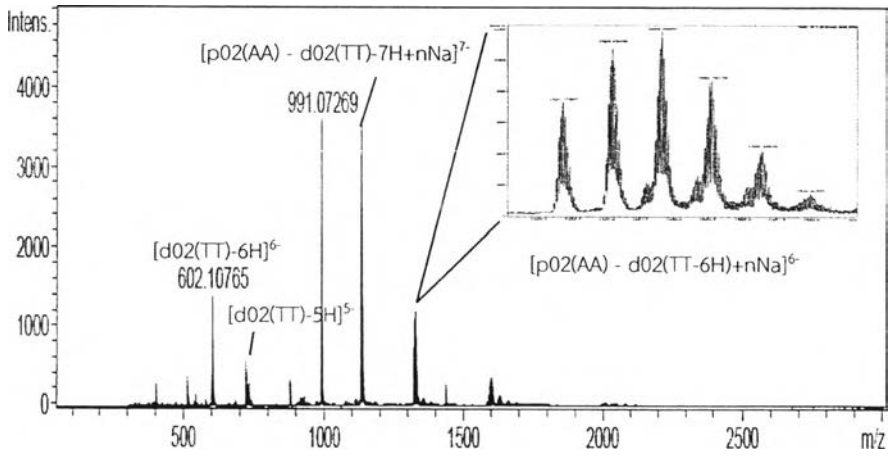

Figure 3.5 Mass spectra of p02 (AA) -d02 (TT) duplex, showing the multiple charged species obtained.

According to Figure 3.5, the experimental molecular mass of p02(AA)–d02(TT) complex was 8001.7006 Da ± 4.8444 ppm (3Na adduct). All peaks of the charges 6-

duplexes at m/z = 1325.4543, 1329.1184, 1332.7832 and 1336.4363 can be interpreted as $[p02(AA)-d02(TT)-6H+Na]^{6-}$, $[p02(AA)-d02(TT)-6H+2Na]^{6-}$, $[p02(AA)-d02(TT)-6H+3Na]^{6-}$ and $[p02(AA)-d02(TT)-6H+4Na]^{6-}$, respectively. All peaks of the charges 7^- duplexes at m/z = 1132.8163, 1135.9605, 1139.0963, 1142.2356 and 1145.2417 can be interpreted as $[p02(AA)-d02(TT)-7H]^{7-}$, $[p02(AA)-d02(TT)-7H+ Na]^{7-}$, $[p02(AA)-d02(TT)-7H+2Na]^{7-}$, $[p02(AA)-d02(TT)-7H+3Na]^{7-}$ and $[p02(AA)-d02(TT)-7H+4Na]^{7-}$ respectively. The peak of free PNA can be observed at m/z = 1438.0182 which corresponds to $[p02\ (AA)-3H]^{3-}$. The peaks of free DNA at m/z = 722.7372, 602.1134 and 515.9541 can be interpreted as $[d02(TT)-5H]^{5-}$, $[d02(TT)-6H]^{6-}$ and $[d02(TT)-7H]^{7-}$, respectively.

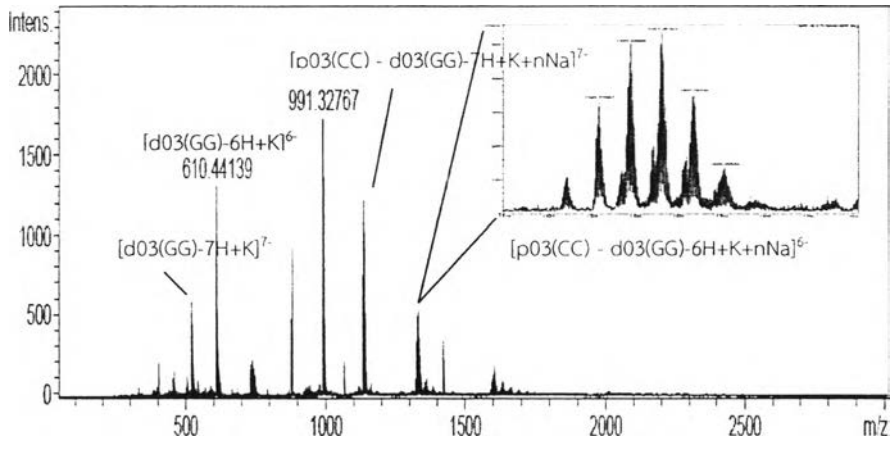

Figure 3.6 Mass spectra of p03 (CC) -d03 (GG) duplex, showing the multiple charged species obtained.

According to Figure 3.6, the experimental molecular mass of p03(CC)–d03(GG) complex was 8002.5456 Da ± 2.6261 ppm (K and 3Na adduct). All peaks of the charges 6^- duplexes at m/z = 1325.7695, 1329.4312, 1333.0933 and 1336.7559 can be interpreted as $[p03(CC)-d03(GG)-6H+K+2Na]^{6-}$, $[p03(CC)-d03(GG)-6H+K+3Na]^{6-}$ and $[p03(CC)-d03(GG)-6H+K+4Na]^{6-}$, respectively. All peaks of the charges 7^- duplexes at m/z = 1136.2283, 1139.3682, 1142.5086 and 1145.6357 can be interpreted as $[p03(CC)-d03(GG)-6H+K+2Na]^{7-}$, $[p03(CC)-d03(GG)-6H+K+3Na]^{7-}$ and $[p03(CC)-d03(GG)-6H+K+4Na]^{7-}$, respectively. The peaks of the free PNA at m/z = 1431.9911 and 1066.4904 can be interpreted as $[p03(CC)-3H]^{3-}$ and $[p03(CC)-4H]^{4-}$. The peaks of free DNA at m/z = 610.4412 and 523.0919 can be interpreted as $[d03(GG)-6H+K]^{6-}$ and $[d03(GG)-7H+K]^{7-}$.

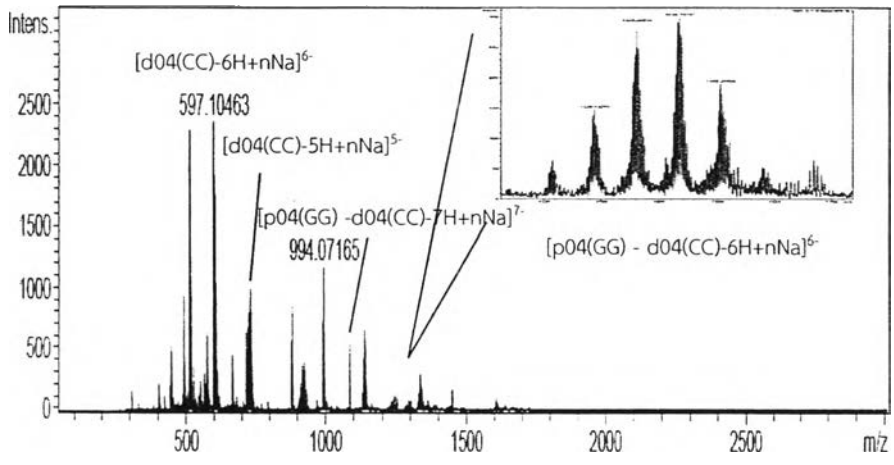

Figure 3.7 Mass spectra of p04 (GG) -d04 (CC) duplex, showing the multiple charged species obtained.

According to Figure 3.7, the experimental molecular mass of p04(GG)–d04(CC) complex was 8003.5836 Da ± 3.1509 ppm (3Na adduct). All peaks of the charges 6^- duplexes at m/z = 1329.4339, 1333.0872 and 1336.7596 can be interpreted as [p04 (GG)-d04(CC)-6H+2Na]$^{6-}$, [p04(GG)-d04(CC)-6H+3Na]$^{6-}$ and [p04(GG)-d04(CC)-6H+4Na]$^{6-}$, respectively. All peaks of the charges 7^- duplexes at m/z = 1136.0877, 1139.3668, 1142.5022 and 1145.6499 can be interpreted as [p04(GG)-d04(CC)-7H+Na]$^{7-}$, [p04(GG) -d04(CC)-7H+2Na]$^{7-}$, [p04(GG)-d04(CC)-7H+3Na]$^{7-}$ and [p04(GG)-d04(CC)-7H+4Na]$^{7-}$, respectively. The peaks of free PNA were observed at m/z = 1448.6594 and 1086.2414 which can be interpreted as [p04(GG)-3H]$^{3-}$ and [p04(GG)-4H]$^{4-}$. The peaks of free DNA (charge 4^-) at m/z = 912.6430, 918.1369, 923.6348 and 929.1280, can be interpreted as [d04(CC)-4H+3Na]$^{4-}$, [d04(CC)-4H+4Na]$^{4-}$, [d04(CC)-4H+5Na]$^{4-}$ and [d04 (CC)-4H+6Na]$^{4-}$, respectively. The peaks of free DNA (charge 5^-) at m/z = 716.7269, 721.1211, 725.5182, 729.9153, 734.3108 and 738.7053, can be interpreted as [d04 (CC)-5H]$^{5-}$, [d04(CC)-5H+Na]$^{5-}$, [d04(CC)-5H+2Na]$^{5-}$, [d04(CC)-5H+3Na]$^{5-}$, [d04(CC)-5H+4 Na]$^{5-}$ and [d04(CC)-5H+5Na]$^{5-}$ respectively. The peaks of free DNA (charge 6^-) at m/z = 597.1045, 600.7687, 604.4327, 608.0948 and 611.7567 can be interpreted as [d04(CC)-6H]$^{6-}$, [d04(CC)-6H+Na]$^{6-}$, [d04(CC)-6H+2Na]$^{6-}$, [d04(CC)-6H+3Na]$^{6-}$ and [d04(CC)-6H+4Na]$^{6-}$, respectively. The peaks of free DNA (charge 7^-) at m/z = 511.6607, 514.8011, 517.9419 and 521.0838 can be interpreted as [d04(CC)-7H]$^{7-}$, [d04(CC)-7H+Na]$^{7-}$, [d04(CC)-7H+2Na]$^{7-}$ and [d04(CC)-7H+3Na]$^{7-}$, respectively. The peaks of free DNA (charge 8^-) at m/z = 447.5781 and 450.3259 can be interpreted as [d04(CC)-8H]$^{8-}$ and [d04(CC)-8H+Na]$^{8-}$, respectively.

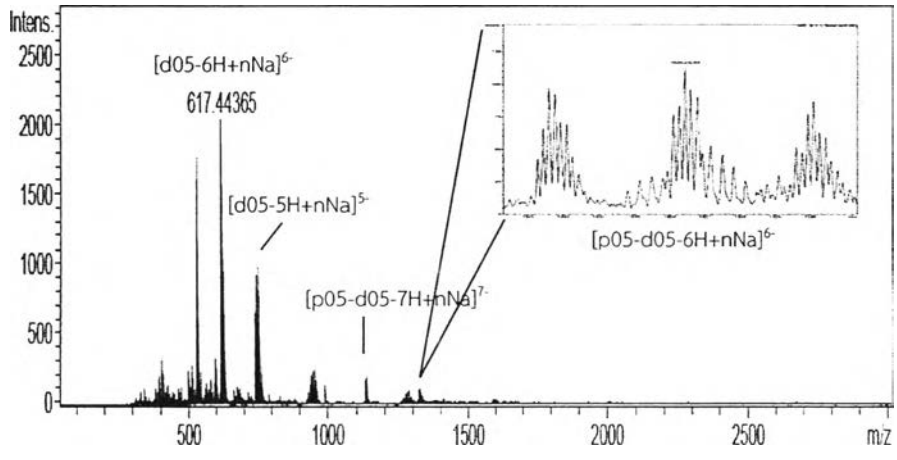

Figure 3.8 Mass spectra of p05-d05 duplex, showing the multiple charged species obtained.

According to Figure 3.8, the experimental molecular mass of p05–d05 complex was 8007.5862 Da ± 4.5740 ppm (3Na adduct). All peaks of the charges 6^- duplexes at m/z = 1322.3925, 1326.4256 and 1330.2572, can be interpreted as $[p05\text{-}d05\text{-}6H]^{6-}$, $[p05\text{-}d05\text{-}6H+Na]^{6-}$ and $[p05\text{-}d05\text{-}6H+2Na]^{6-}$ respectively. All peaks of the charged 7^- duplexes at m/z = 1133.6486, 1136.7994 and 1139.9277 can be interpreted as $[p05\text{-}d05\text{-}7H]^{7-}$, $[p05\text{-}d05\text{-}7H+Na]^{7-}$ and $[p05\text{-}d05\text{-}7H+2Na]^{7-}$, respectively. The peaks of free DNA (charge 4^-) at m/z = 943.6524, 948.6398, 954.1362 and 959.6317, can be interpreted as $[d05\text{-}4H+3Na]^{4-}$, $[d05\text{-}4H+4Na]^{4-}$, $[d05\text{-}4H+5Na]^{4-}$ and $[d05\text{-}4H+6Na]^{4-}$ respectively. The peaks of free DNA (charge 5^-) at m/z = 741.1255, 745.5225, 749.9188, 754.3139, 758.7105 and 763.1096 can be interpreted as $[d05\text{-}5H]^{5-}$, $[d05\text{-}5H+Na]^{5-}$, $[d05\text{-}5H+2Na]^{5-}$, $[d05\text{-}5H+3Na]^{5-}$, $[d05\text{-}5H+4Na]^{5-}$ and $[d05\text{-}5H+5Na]^{5-}$, respectively. The peaks of free DNA (charge 6^-) at m/z = 617.4373, 521.0997, 624.7641 and 628.4276 can be interpreted as $[d05\text{-}6H]^{6-}$, $[d05\text{-}6H+Na]^{6-}$, $[d05\text{-}6H+2Na]^{6-}$ and $[d05\text{-}6H+3Na]^{6-}$, respectively.

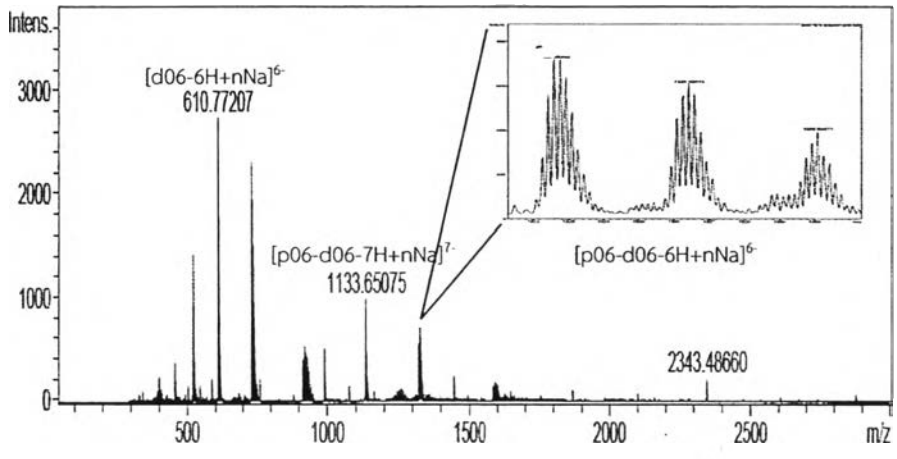

Figure 3.9 Mass spectra of p06-d06 duplex, showing the multiple charged species obtained.

According to Figure 3.9, the experimental molecular mass of p06–d06 complex was 7961.6376 Da ± 0.7541 (Na adduct). All peaks of the charges 6^- duplexes at m/z = 1322.6057, 1326.4274 and 1330.2507, can be interpreted as $[p06\text{-}d06\text{-}6H]^{6-}$, $[p06\text{-}d06\text{-}6H+Na]^{6-}$ and $[p06\text{-}d06\text{-}6H+2Na]^{6-}$, respectively. All peaks of the charged 7^- duplexes at m/z = 1133.5111, 1136.7954 and 1140.0734 can be interpreted as $[p06\text{-}d06\text{-}7H]^{7-}$, $[p06\text{-}d06\text{-}7H+Na]^{7-}$ and $[p06\text{-}d06\text{-}7H+2Na]^{7-}$, respectively. The peaks of free PNA at m/z = 1422.6576 corresponds to $[p06\text{-}3H]^{3-}$. The peaks of free DNA (charge 4^-) at m/z = 916.6648, 922.1625, 927.6572 and 933.1520 are assigned as $[d06\text{-}4H]^{4-}$, $[d06\text{-}4H+Na]^{4-}$, $[d06\text{-}4H+2Na]^{4-}$ and $[d06\text{-}4H+3Na]^{4-}$, respectively. The peaks of free DNA (charge 5^-) at m/z = 733.1330, 737.5288, 741.9258 and 746.3224 can be interpreted as $[d06\text{-}5H]^{5-}$, $[d06\text{-}5H+Na]^{5-}$, $[d06\text{-}5H+2Na]^{5-}$ and $[d06\text{-}5H+3Na]^{5-}$, respectively. The peaks of DNA (charge 6^-) at m/z = 610.7784, 614.4411 and 618.1034, can be interpreted as $[d06\text{-}6H]^{6-}$, $[d06\text{-}6H+Na]^{6-}$ and $[d06\text{-}6H+2Na]^{6-}$, respectively.

The results of the analysis showed the peaks of acpcPNA-DNA complexes with charge 6^- and 7^- as the major species in all mass spectra. because the charge 6^- is more stable than the charge 7^- when increasing the collision energy. Since the charge 6^- is more stable than the charge 7^- species at increasing collision energy, we will choose to study energy of all acpcPNA-DNA complexes at charge 6^- by CID technique.

3.3 Studies of noncovalent interaction in PNA-DNA duplexes

The energy of noncovalent interaction between PNA and DNA was studied by collision induced dissociation (CID). The PNA-DNA complexes dissociate upon increasing the energy applied to ionize the complexes. The stability of the PNA-DNA complexes can be estimated from the dissociation energy, which can be obtained according to the equation $E_{CM} = E_{LAB}\ [m_g/(m_g+m_p)]$ (E_{CM} = center-of-mass collision energy, E_{LAB} = ZeV (z = number of charge) = ion kinetic energy in the laboratory frame, m_g = mass of the stationary target gas , m_p = mass of projectile ion). In each spectrum, the duplex ions appear at two charge states (7^- and 6^-) with the former being more prevalent. Under gentle CID conditions in the ESI, we find that dissociation of the 6^- duplex into its constitutive single strands is the major pathway because the 6^- duplex is more stable than other peak. Therefore, we report the CID experiments on the 6^- charged duplexes only. The dissociation of the parent duplexes ion is monitored by the disappearance of the duplex signal and the appearance of the single strands. The dissociation profiles of six duplexes are displayed in Figure 3.10 - Figure 3.15.

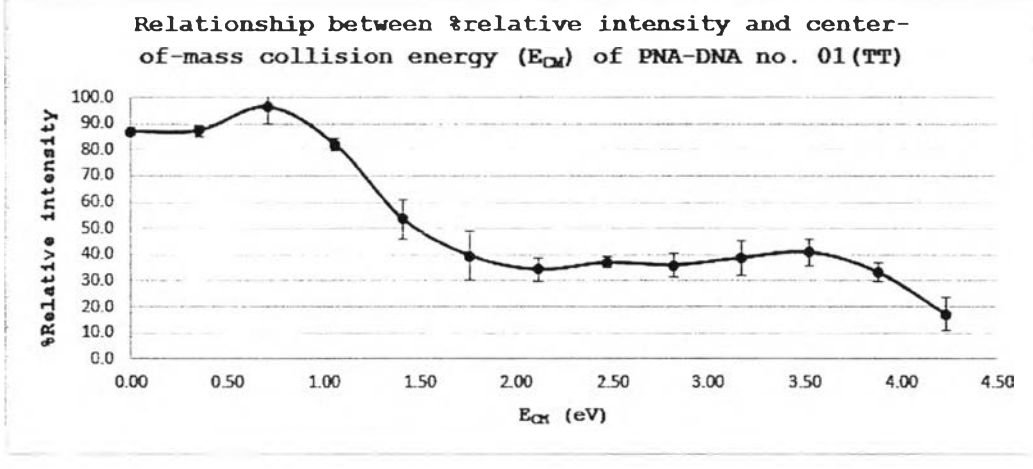

Figure 3.10 Relationship between energy and relative intensity of duplex p01 (TT)-d01(AA). The relative intensity relate with ion abundance of duplex ion.

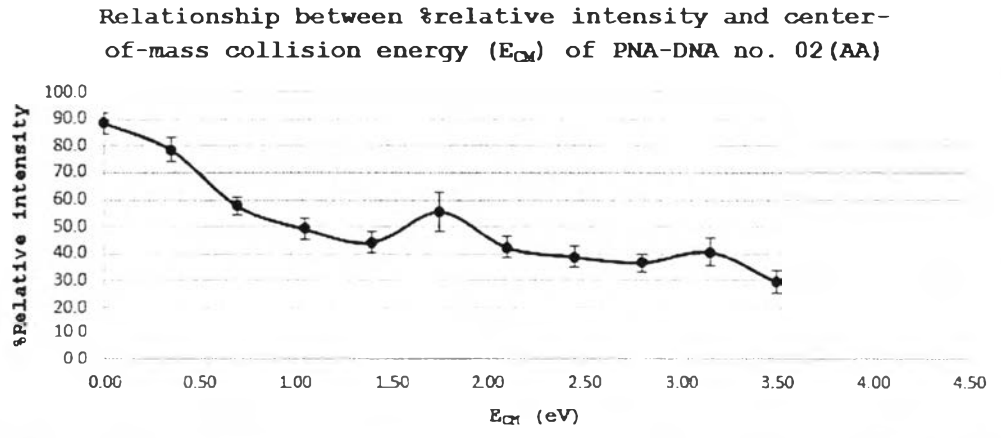

Figure 3.11 Relationship between energy and relative intensity of duplex p02 (AA)-d02(TT). The relative intensity relate with ion abundance of duplex ion.

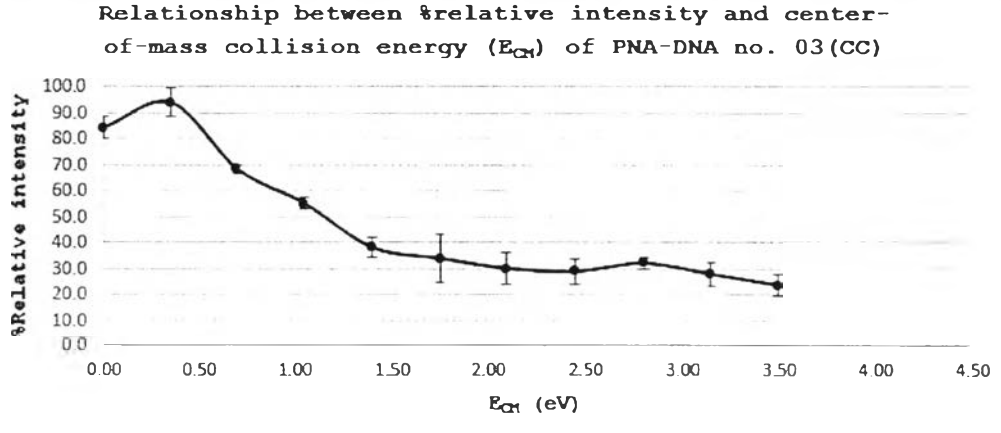

Figure 3.12 Relationship between energy and relative intensity of duplex p03 (CC)-d03(GG). The relative intensity relate with ion abundance of duplex ion.

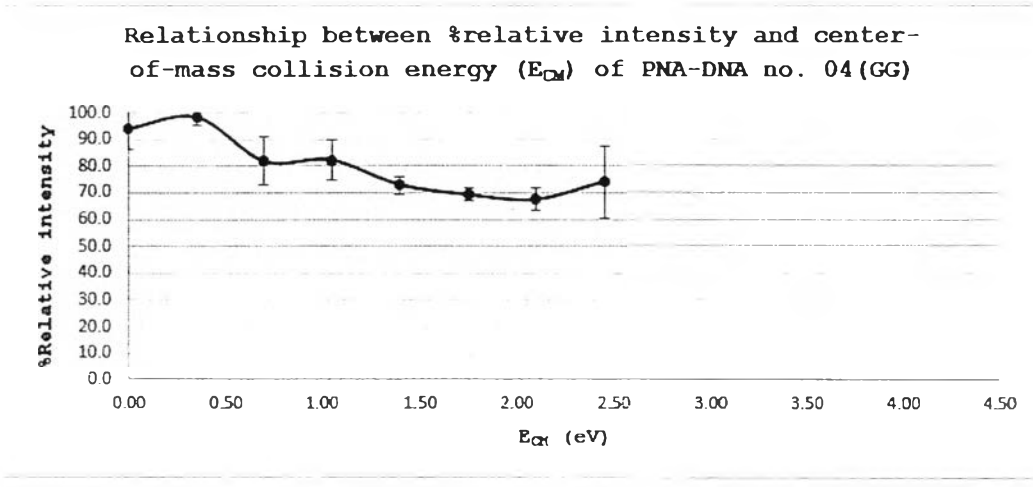

Figure 3.13 Relationship between energy and relative intensity of duplex p04 (GG)-d04(CC). The relative intensity relate with ion abundance of duplex ion.

The energy of the first set of acpcPNA-DNA complexes was shown in Figure 3.10 - Figure 3.13. According to the E_{CM} values, the relative stability of PNA-DNA complexes can be ranked as follows: p01 (TT) = 4.22 eV > p02 (AA) = 3.49 eV ≈ p03 (CC) = 3.49 eV > p04 (GG) = 2.44 eV, respectively.

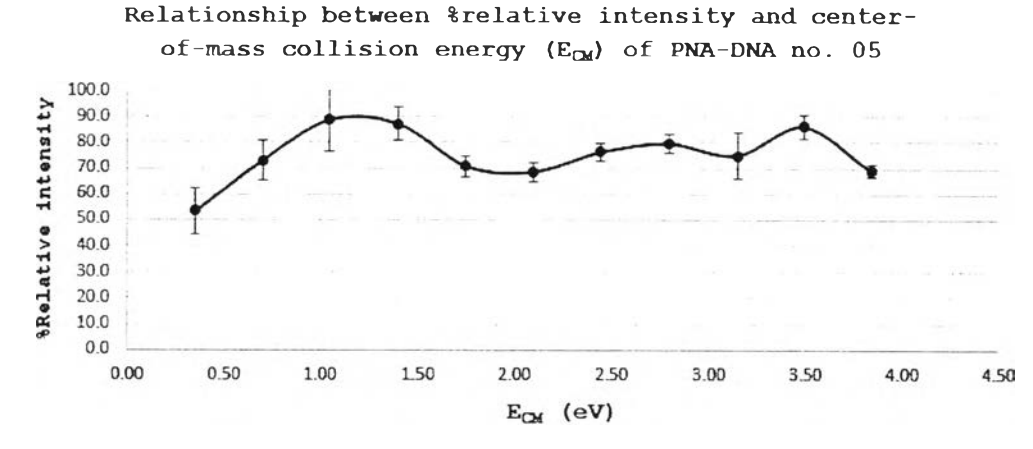

Figure 3.14 Relationship between energy and relative intensity of duplex p05-d05. The relative intensity relate with ion abundance of duplex ion.

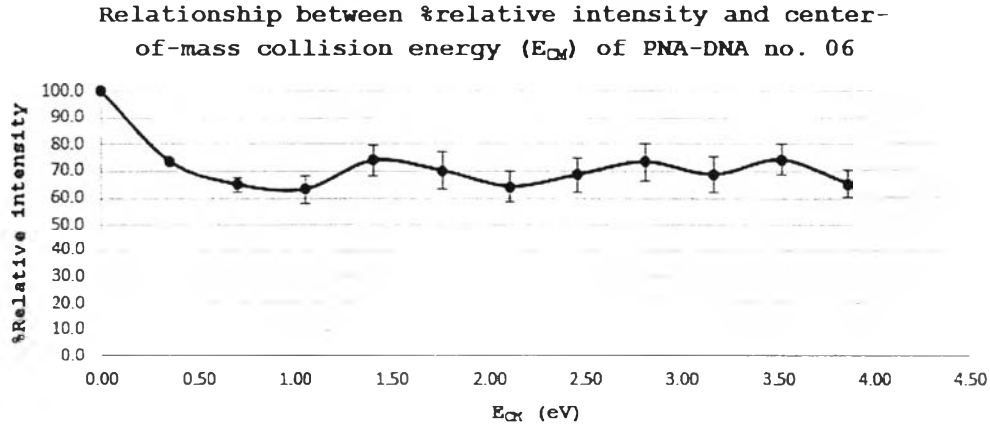

Figure 3.15 Relationship between energy and relative intensity of duplex p06-d06. The relative intensity relate with ion abundance of duplex ion.

According to Figure 3.14 - Figure 3.15, the E_{CM} value of p05-d05 and p06-d06 complexes were detected at 3.84 eV and 3.86 eV, respectively.

3.4. Stability of PNA-DNA duplexes in solution phase versus gas phase

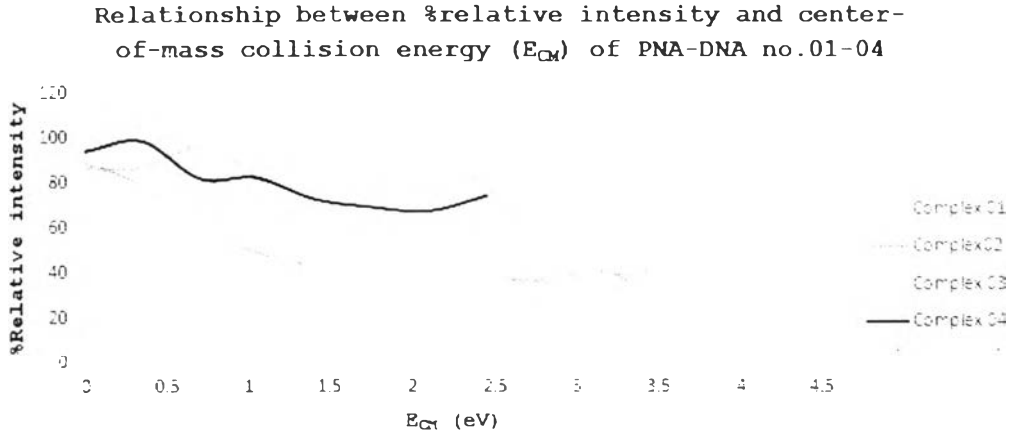

Figure 3.16 The relationship between energy of and relative intensity of hybrids of p01 (TT), p02 (AA), p03 (CC), p04 (GG) with their complementary DNA (charge 6-). The relative intensity relate with ion abundance of duplex ion.

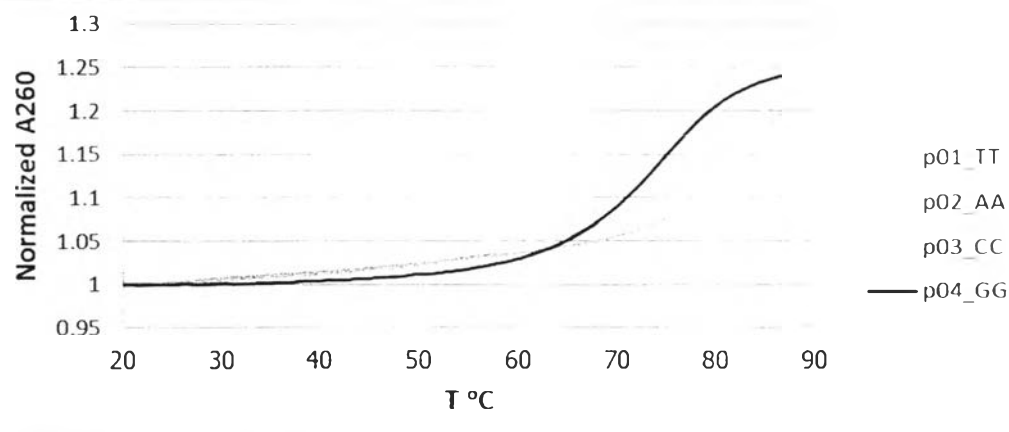

Figure 3.17 Melting curves of hybrids of p01 (TT), p02 (AA), p03 (CC), p04 (GG) with their complementary DNA (measured at 260 nm, in 10 mM sodium phosphate buffer, pH 7.0 at 1 μM concentration).

Table 3.2 Energy and melting temperature value of PNA-DNA complexes

PNA/DNA no.	PNA/DNA Seq.	E_{CM}	$E_{1/2}$	T_m
p01 (TT)	TGT TAATTG ACT	4.2280	2.114	> 82.5
d01 (AA)	ACA ATTAAC TGA			
p02 (AA)	TGT AAAATG ACT	3.4938	1.7469	82.5
d02 (TT)	ACA TTTTAC TGA			
p03 (CC)	TGT CAACTG ACT	3.4934	1.7467	69.5
d03 (GG)	ACA GTTGAC TGA			
p04 (GG)	TGT GAAGTG ACT	2.4451	1.2225	74.1
d04 (CC)	ACA CTTCAC TGA			
p_05	CGC GCTCCG CTA	3.8404	1.9202	71.2
d_05	GCG CGAGGC GAT			
p_06	CGC GCAGGT TCC	3.8620	1.9310	70.8
d_06	GCG CGTCCA AGG			

$E_{1/2}$ means half of the E_{CM} value.

The obtained E_{CM}, $E_{1/2}$ and T_m values measured by ESI-MS and UV-vis respectively, are shown in Figures 3.16 – 3.17. Both values are used to compare the stability of noncovalent interaction of PNA-DNA complexes. The E_{CM} values were ordered as p01 (TT) > p02 (AA) ≈ p03 (CC) > p04 (GG), respectively. The T_m values were ordered as p01 (TT) > p02 (AA) > p04 (GG) > p03 (CC), respectively.

Stability of acpcPNA-DNA complexes with T and A bases at positions 4 and 7 in the gas phase corresponds to the T_m values in solution phase because the stability of A-T pairs are dominated by hydrogen bonding. The research of Su Pan and colleagues [45] have described the alternate base pairs on a PNA strand (T-A, A-T, C-G, G-C), it also affects the stability of PNA-DNA complexes. The experimental of Su Pan was studied of the influence of the base stacking affect the stability of PNA-DNA complexes. The stability showed that the duplex AT is less stable than duplex TA in the gas phase. However, the stability of PNA-DNA complexes with G and C bases at the positions 4 and 7 in the gas phase does not correspond to T_m in solution phase

because the stability of G-C pairs depends on both hydrogen bonding and base stacking.

According to Figure 3.16, in the first stages the intensity of PNA-DNA complexes is increased. Due to the transfer the energy from collision gas, the inner energy of PNA-DNA complexes was increased initially as already discussed in 3.1. In the next stage, the intensity was reduced because the inner energy changed to kinetic energy. The PNA-DNA complexes were dissociated by kinetic energy. In addition, the result shows that the PNA strand contains many G bases is not stabilized by the inner energy according to the result from Valérie Gabelica [27]. Consequently, the influences of the inner energy were observed in the order of T > A ≈ C > G, respectively. On the other hand, order of base pair stability in the solution phase were T-A > A-T > G-C > C-G because of the influence of H-bonding and base stacking [46]. The melting curves of hybrids of all acpcPNA-DNA complexes in the solution phase measured at 260 nm in sodium phosphate buffer solution pH 7.0 at 1 μM concentration. We used buffer solution pH 7.0 because the PNA-DNA complex capture well than the acid or base buffer solution [37, 41, 46, 47].

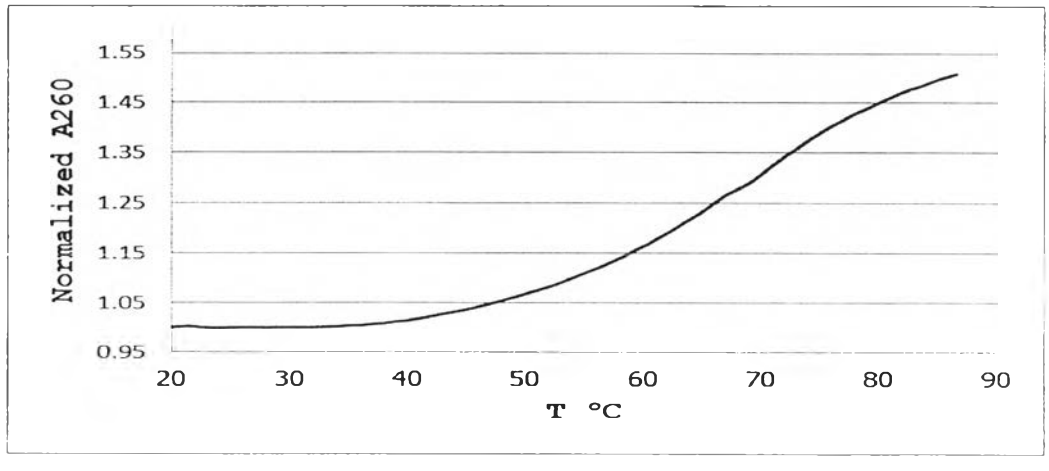

Figure 3.18 Melting curves of hybrids of p05 with its complementary DNA (measured at 260 nm, in 10 mM sodium phosphate buffer, pH 7.0 at 1 μM concentration).

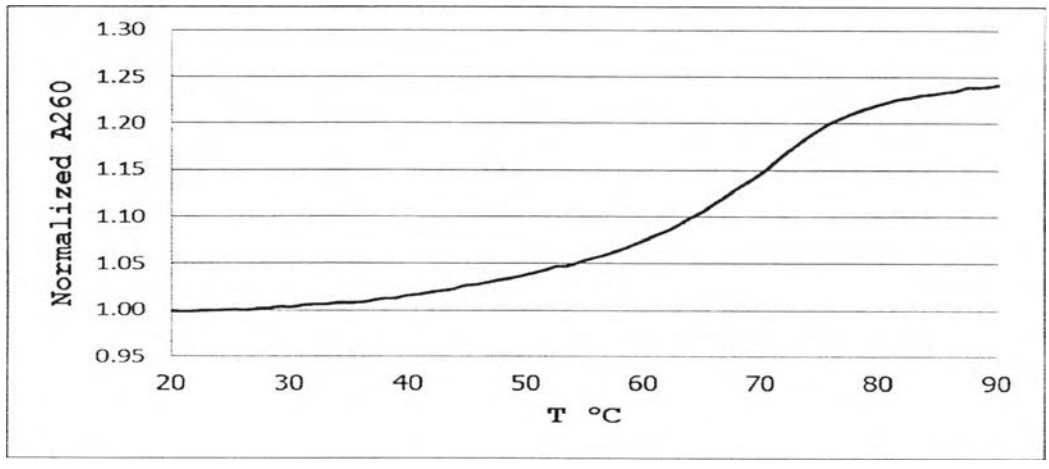

Figure 3.19 Melting curves of hybrids of p06 with its complementary DNA (measured at 260 nm, in 10 mM sodium phosphate buffer, pH 7.0 at 1 μM concentration).

In the second set of PNA, the relative stabilities obtained from gas phase and solution phase experiments are slightly different (Figure 3.18 – Figure 3.19). From the E_{CM} value of the duplex p06-d06 is a little more stable than duplex p05-d05. Because the PNA strand of p06 have more purine base than p05 and the PNA strand of p06 have the terminal G and C base. The terminal G and C base help to maintain the helical structure of PNA-DNA complexes.

In this experiment we are understanding the dissociation kinetics is a prerequisite to interpret MS/MS dissociation pathways. The observation of a given fragmentation pathway depends on whether the precursor ion received sufficient amount of internal energy to undergo fragmentation before the product ion spectrum is recorded. The two key instrumental parameters are the amount of internal energy given in the activation step, and the time allowed for fragmentation (in other words, the fragmentation time scale). Type of fragmentation in a quadrupole time of flight takes place in less than a millisecond (short fragmentation time scale), whereas in a quadrupole ion trap or an FT-ICR-MS/MS it takes from 30 ms to seconds (long fragmentation time scale). Therefore, during the experiment when increasing the internal energy is strand separation. Conversely, when using instruments allowing for long fragmentation time scale, the first reaction pathway observed when increasing the internal energy is base loss.

In this experiment, the restrictions on the parameter that may affect the stability of the complex measurements such as cone voltage parameter. Unfortunately we were unable to modify the cone voltage setting. The setting parameter of high cone voltage will result in a complex separation before increasing the energy to collision cell. So we will see the peak of the DNA strand in the mass spectrum. The ESI-MS experiment can be used to estimate the stability of the noncovalent interaction of PNA-DNA complexes in the gas phase. The data obtained from ESI-MS show that the effect of inner energy to the stability of PNA-DNA complexes. In the most research is related to the use of PNA as a probe to detect DNA sequences. So, we hope that the information from this experiment will be useful in understanding the nature of PNA-DNA interactions.